Research Square

Preprints are preliminary reports that have not undergone peer review.
They should not be considered conclusive, used to inform clinical practice,
or referenced by the media as validated information.

Investigation on the magnetorheological shear thickening finishing with radial slotted magnetic pole for Sine surface

Zhiguang Sun
Zenghua Fan
Yebing Tian (tianyb@sdut.edu.cn)
Shandong University of Technology
Cheng Qian
Zhen Ma

Research Article

Keywords: Sine surface, Radial slotted magnetic pole, Magnetic field assisted finishing, Magnetorheological shear thickening finishing

Posted Date: March 15th, 2022

DOI: https://doi.org/10.21203/rs.3.rs-1431050/v1

License: This work is licensed under a Creative Commons Attribution 4.0 International License.
Read Full License

Investigation on the magnetorheological shear thickening finishing with radial slotted magnetic pole for Sine surface

Zhiguang Sun [1], Zenghua Fan[1, 2], Yebing Tian[1, 2*], Cheng Qian[1], Zhen Ma[1]

[1] School of Mechanical Engineering, Shandong University of Technology, Zibo 255049, P. R. China

[2] Institute for Advanced Manufacturing, Shandong University of Technology, Zibo 255049, P. R. China

---

[*]**Corresponding Author**:

Yebing Tian,
School of Mechanical Engineering,
Shandong University of Technology,
Address: 266 Xincun West Road, Zibo, Shandong 255049, P.R. China,
E-mail: tianyb@sdut.edu.cn; tyb79@sina.com,
Tel: +86 150 5333 1895

Abstract

Free-form surfaces have widespread applications in the fields of integrated circuit, and automobile sectors because of the typical geometric characteristics. Surface finishing of free-form surfaces is a critical process to fulfill target quality. In present study, a magnetorheological shear thickening finishing (MSTF) method is proposed for Sine surface finishing based on the designed finishing tool and the developed MSTF media. The MSTF utilizes a flexible finishing tool, integrating a slotted cylindrical permanent magnetic pole with radial magnetization, is fabricated to dominate rheological properties of finishing media to guarantee the finishing force. To obtain sufficiently large magnetic flux density and magnetic field gradients in the finishing zone, finite element analysis (FEA) is used to obtain the optimal dimensions and structure of the finishing tool. The principle of the method is illustrated and mathematical model of material removal is established. Finishing experiments were conducted on Sine surface fabricated by SUS304 based on the developed MSTF media and the established platform. The effects of finishing parameters on surface roughness are evaluated quantitatively. The results substantiate that the material was uniformly re-moved over the entire Sine surface and the developed method is capable for Si-ne finishing with a more than 87% improvement in surface roughness. The method in the paper shows signs of future success in finishing free-form surfaces in a wide range of industrial applications.

Keywords: Sine surface, Radial slotted magnetic pole, Magnetic field assisted finishing, Magnetorheological shear thickening finishing

1 Introduction

Free-form surfaces have widespread applications in biomedical engineering industry, integrated circuit industry and automotive manufacturing. Fang et al. [1] thought that more rigorous requirements for the surface quality of free-form surfaces were presented with the rapid development of manufacturing technology. The finishing process became a critical factor in improving the quality of free-form surfaces. Zhang et al. [2] summarized the existing ultra-precision machining methods and thought that traditional finishing methods were difficult to meet the rigorous requirements including higher surface roughness and lower shape accuracy. Xia et al. and Yuan et al. [3, 4] made comprehensive reviews of ultra-precision machining technology, in which non-traditional finishing methods aimed at enhancing surface roughness and shape accuracy of free-form surfaces were highlighted, i.e. abrasive flow polishing (AFM), laser polishing, magnetic field assisted finishing (MFAF) and magnetorheological finishing (MRF), etc.

The finishing processes for free-form surfaces were developed in previous literatures. Yung et al. [5] presented a method to reduce the surface roughness of Cobalt Chromium (CoCr) parts with complex geometry using laser polishing. The surface roughness was improved by 93% with optimal polishing parameters. Wu et al. [6] proposed a polishing technique for sphere polishing by grinding center with an elastic ball type wheel. The polishing characteristics of workpiece with different processing parameters were investigated. The polished profiles of sphere were predicted by the finite element analysis (FEA), which showed a good agreement with experiment results. Zhao et al. [7] focused on the study of oblique ultrasonic polishing mechanism for free-form surface. The mechanical model and kinematics model of the finishing process were established. Sarkar et al. [8] reported rotational-magnetorheological abrasive flow

finishing for knee joint implant surface finishing which combined the AFM and MFAF technology. By optimizing finishing parameters, non-uniform surface roughness ranging from 35 nm to 78 nm was obtained at different locations of the knee joint implant. In addition, Tam et al. [9] focused on mechanical polishing for free-form surfaces by robotic trajectory planning, which improved finishing efficiency and surface quality.

The MFAF method employs a magnetic brush formed under magnetic field as a finishing tool. Magnetic brush exhibits good flexibility and self-adaptive, which enables access to the finishing zone that is hard to reach by traditional finishing methods. Therefore, the MFAF method is widely used for finishing of various surfaces. Recently, Qian et al. and Singh et al. [10, 11] reported various kind of the developed MFAF method for free-form surface finishing. The finishing tool and finishing media have become critical factors affecting the performance of MFAF. Singh et al. [12] made a comprehensive review for the magnetic abrasives fabrication by sintering, adhesion, and mechanical mixing. Zhang et al. [13] developed an iron-based SiC spherical composite magnetic abrasive using gas atomization and rapid solidification. The sintered magnetic abrasive exhibited a high material removal rate (MRR) and longer finishing life. However, the wider application of sintered magnetic abrasive was limited by the complex fabrication process and high production costs. Zhang et al. [14] developed a finishing tool with bonded abrasive coating for the inner surface finishing of round tube, in which abrasive particles and the finishing tool were bonded by glue. The feasibility of the proposed finishing method was verified using experiments. Free magnetic abrasives had unique dominance over bonded magnetic abrasives in terms of nano finishing processes. Guo et al. [15] conducted finishing experiments on the double-layered internal surface finishing fabricated by Inconel 718 selective laser melting using a finishing media contained stainless steel (SS430) cut-ting wire, SiC particles and machining oil. The surface roughness of inner surface reduced from 7 μm to 1 μm

with the improvement the hardness and residual stress. Fan et al. [16] developed an intelligent finishing media by combining shear thickening fluids (polyethylene glycol and fumed silica), SiC abrasives, Carbonyl iron particles (CIPs). Finishing experiments were conducted on Ti-6Al-4V workpiece, which demonstrated that the enhanced finishing media could achieve nano-level surface finishing.

The magnetic field in the finishing zone is dominated by the magnetic field apparatus. Some researches focused on the optimization of magnetic field apparatus. Fan et al. [17] designed a four-pole rotating magnetic field generation device based on the multipole coupling effect. The finishing experiments on Ti-6Al-4 V workpieces were conducted. The minimum surface roughness of 46 nm was obtained from initial 1.121 μm under optimal finishing parameters. Jiao et al. [18] developed a magnetic generator for surface finishing of seal ring grooves based on the finite element analysis (FEA) of magnetic field. The target surface roughness of the ring groove with the optimal finishing parameters was decreased to 0.6 μm from original 4.3 μm improving over 86%. Singh et al. [19] developed finishing tool with a ball end using electro-magnetic coils. The surface roughness of grooves was decreased to 102 nm from initial 336.8 nm in 60 min. Guo et al. [20] established vibration-assisted magnetic abrasive polishing (VAMAP) platform for polishing rectangular microfeatures, and investigated the critical conditions of the VAMAP process in polishing rectangular microfeatures. Tool marks caused by micro milling were completely removed. The surface morphology, roughness and profile were quantitatively evaluated before and after polishing for comparison. To improve the efficiency and surface quality of free-form surface polishing, Wang et al. [21] developed the magnetic field-assisted mass polishing (MAMP) system with four sets of symmetrical permanent magnetic poles. The optimal surface roughness (Sa) of 13.8 nm was achieved from initial 455.4 nm for 304 stainless steel workpiece. Similarly, Prakash et al. [22] described the effects of the MAF for polishing the

high strength biomedical grade b-phase TieNbeTaeZr (b-TNTZ) alloy on orthopedic applications. An angle-adjustable permanent magnetic pole with axial magnetization was designed as finishing tool. The change of surface roughness (%ΔRa) of workpiece reached by 97.68%. From the available researches, it is observed that few researchers are interested in the finishing tool developed with the changing magnetization direction of permanent magnetic poles for Sine surfaces finishing.

In the present study, an enhanced magnetorheological shear thickening finishing (MSTF) method is proposed to finishing Sine surface of SUS304. The FEA method based COMSOL simulation approach is used to determine the optimal shape and dimension of the radial permanent magnetic pole. The MSTF media are prepared by the combination of CIPs and CBN abrasives in a base mixture of polyethylene glycol (PEG 200) and fumed SiO_2 silica (SiO_2). Finishing experiments are carried out to verify the feasibility of the MSTF method. The effects of various components of the MSTF media, spindle rotational speed and working gap on surface quality are systematically analyzed.

2 Principles

Fig. 1 shows a principle of the MSTF using a MSTF media consisting of CIPs, CBN abrasives, PEG 200 and SiO_2. The working gap between the lateral side of finishing tool and Sine surface is filled with the MSTF media under the influence of the magnetic field generated by the radial slotted magnetic pole. Relative motion between the MSTF media and Sine surface is formed by controlling the movement of workpiece and rotation of finishing tool. As shown in Fig. 1(b), some chains along the magnetic lines at the lateral side of finishing tool are formed by the CIPs of the MSTF media which results in a sudden increase in the apparent viscosity of the MSTF media in the finishing zone. It is called magnetorheological (MR) effect. When relative

motion is provided between the MSTF media and the Sine surface, the shear thickening effect appears because the micro-convex peaks on the Sine surface blocks the motion of MSTF media causing the shear rate changes of the MSTF media. The micro-convex peaks on the Sine surface are removed in the form of microchips under the combined the MR effect and shear thickening effect, as shown in Fig. 1(c). Then, the magnetic abrasives return to the initial configuration, completing the cycle of the media, as shown in Fig. 1(d).

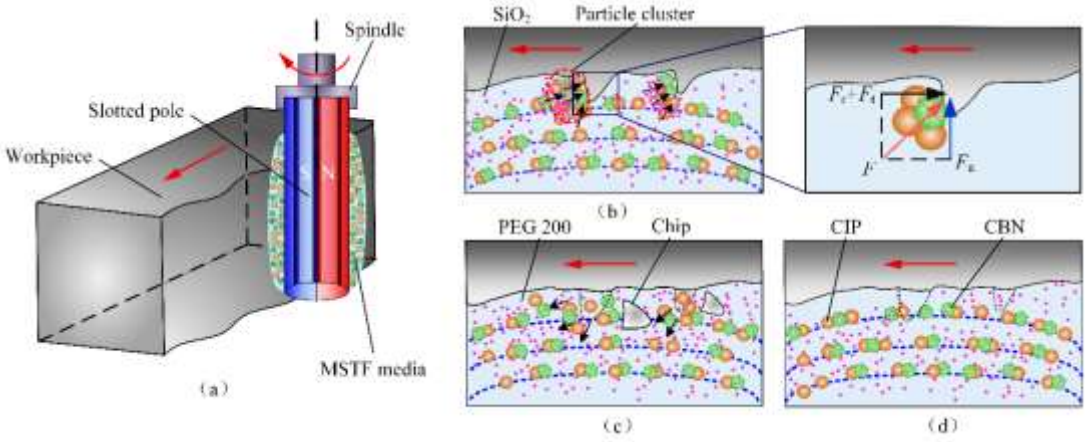

Fig. 1. Principle of the MSTF for Sine surfaces. (a) Three-dimensional schematic, (b) generated particle clusters, (c) removed micro-peaks, and (d) recovery status

3 Mathematical model

In the MSTF process, the finishing force is the most important factor affecting the surface finishing. The resultant finishing force, as shown in Fig. 1(b), is generated by combination of the MR effect and shear thickening effect, which is given by F as follow

$$F = \sqrt{\left[\left(F_r + F_t\right)^2 + F_n^2\right]} \tag{1}$$

Where, F_r is shear force due to the shear thickening effect; F_n and F_t are the normal force and tangential force generated by magnetic abrasives under the action of the magnetic field, respectively.

Assuming that single magnetic abrasive of the MSTF media is a standard cube, which consists of mixture (PEG 200 and SiO_2), CIPs and CBN abrasives, as shown in Fig. 2(a). Single magnetic abrasive is placed in an inhomogeneous magnetic field, as shown in Fig. 2(b). The magnetic force on single magnetic abrasive is equal to the vector sum of the magnetic forces acting on each side. The magnetic forces on both left and right sides are cancelled each other because of the symmetry of magnetic field and magnetic abrasive particle on the horizontal plane. According to the Lorentz force and Maxwell′ s Electromagnetic Force Equations [23], the formulas of magnetic force F_{y1} on the side of high magnetic field intensity and magnetic force F_{y2} on the side of low magnetic field intensity are shown in Eqs. (2) and (3), respectively.

$$F_{y1} = \mu_m \frac{S_1}{2} H_{y1}^2 \tag{2}$$

$$F_{y2} = \mu_m \frac{S_2}{2} H_{y2}^2 \tag{3}$$

Where, μ_m is magnetic permeability of the MSTF media; S_1 and S_2 are the bottom and top sizes of single magnetic abrasive, respectively; H_1 and H_2 are magnetic field intensity at the bottom and top sides of single magnetic abrasive, respectively.

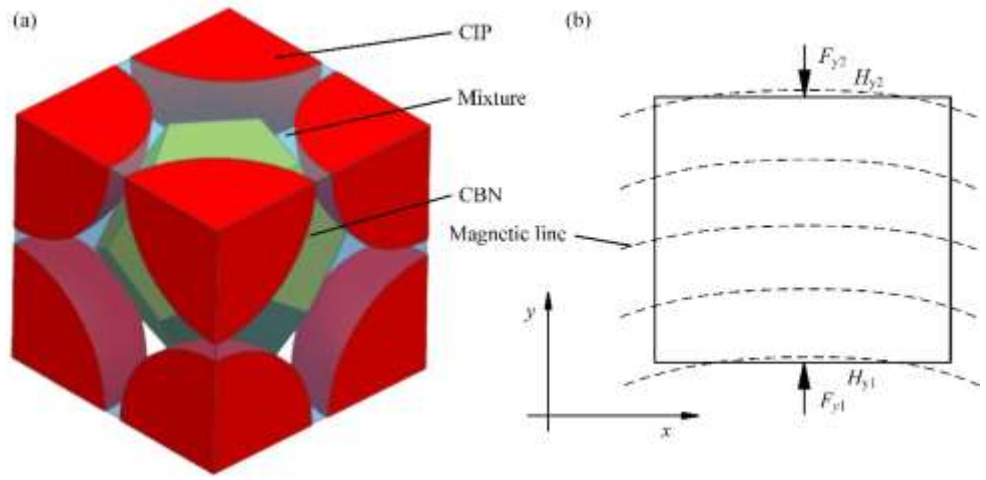

Fig. 2. Schematic diagram of the structure and forces on single magnetic abrasive. (a) Model of single magnetic abrasive, (b) magnetic force of magnetic abrasive in magnetic field

The formula of combined force F_y for the magnetic abrasive is as follow

$$F_y = F_{y1} - F_{y2} = \mu_m \frac{S_1}{2}\left(H_{y1}^2 - H_{y2}^2\right) \tag{4}$$

The magnetic field of the MSTF media is generated by the magnetic field apparatus. Considering the magnetic flux leakage, the relationship between H_{y1} and H_{y2} is given as follow

$$H_{y1} = H_{y2} + \mu_m \frac{\partial H}{\partial y}\frac{V}{S_1} \tag{5}$$

Where, $\frac{\partial H}{\partial y}$ is the magnetic field gradients along the y direction in finishing zone; V is the volume of single magnetic abrasive.

Eq. (6) is obtained by substituting Eq. (5) into Eq. (4), as follow

$$F_y = \mu_m \frac{S_1}{2}\left[\left(\mu_m \frac{\partial H}{\partial y}\frac{V}{S_1}\right)^2 + 2H_{y2}\frac{\partial H}{\partial y}\frac{V}{S_1}\right] \tag{6}$$

The volume of magnetic abrasive is much smaller than the other parameters, then $\left(\mu_m \frac{\partial H}{\partial y}\frac{V}{S_1}\right)^2 \to 0$, Eq. (7) is given as follow

$$F_y = \mu_m V H_{y2} \frac{\partial H}{\partial y} \tag{7}$$

According to Eq. (7), the magnetic permeability of magnetic abrasive can be obtained as

$$\mu_m V H \frac{\partial H}{\partial y} = \mu_a V_a H \frac{\partial H}{\partial y} + \mu_b V_b H \frac{\partial H}{\partial y} + \mu_c V_c H \frac{\partial H}{\partial y} \tag{8}$$

By organizing Eq. (8), Eq. (9) is obtained as follow

$$\mu_m = \mu_a V_a' + \mu_b V_b' + \mu_c V_c' \tag{9}$$

Where, μ_a, μ_b and μ_c are magnetic permeability of CIP, CBN particle and mixture (PEG 200 and SiO_2), respectively; V_a, V_b and V_c are actual volume of CIPs, CBN abrasives and mixture in single magnetic abrasive, respectively; V_a', V_b' and V_c' are the percentage of volume for CIPs, CBN abrasives and mixture in single magnetic abrasive, respectively; and, $V = V_a + V_b + V_c$, $V_a' + V_b' + V_c' = 1$.

Eq. (10) is given combining Eqs. (7) and (9) as follow

$$F_y = \left(\mu_a V_a' + \mu_b V_b' + \mu_c V_c'\right) V H_{y2} \frac{\partial H}{\partial y} \tag{10}$$

On basis of Eq. (10), Eqs. (11) and (12), the normal force F_n and tangential force F_t are obtained as follows

$$F_n = \left(\mu_a V_a' + \mu_b V_b' + \mu_c V_c'\right) VH \frac{\partial H}{\partial n} \tag{11}$$

$$F_t = \left(\mu_a V_a' + \mu_b V_b' + \mu_c V_c'\right) VH \frac{\partial H}{\partial t} \tag{12}$$

Where, H is magnetic field intensity in finishing zone; $\frac{\partial H}{\partial n}$ and $\frac{\partial H}{\partial t}$ are magnetic field gradients along the normal and tangential direction in finishing zone, respectively.

In this paper, the prepared MSTF media is a non-Newtonian fluid. According to law of Newton inner friction [24], the relationship between shear stress and viscosity can be expressed as following

$$\tau = u\delta \tag{13}$$

Where, τ is the shear stress of MSTF media; u and δ are gradients of velocity and viscosity, respectively.

Therefore, F_r is given as follow

$$F_r = u\delta A \tag{14}$$

Where, A is the contact area between the MSTF media and the target surface.

Combining Eqs. (1), (11), (12) and (14), F is obtained as follow

$$F=\sqrt{\left\{\left[u\delta A+\left(\mu_a V_a'+\mu_b V_b'+\mu_c V_c'\right)VH\frac{\partial H}{\partial t}\right]^2+\left[\left(\mu_a V_a'+\mu_b V_b'+\mu_c V_c'\right)VH\frac{\partial H}{\partial n}\right]^2\right\}} \quad (15)$$

On the basis of the Preston equation (Preston, 1927), the average MRR of the finishing zone is calculated as follow

$$\begin{aligned} MRR &= KPv \\ &= KN\left(n\pi d+v_f\right)\left\{\frac{\sqrt{\left[u\delta A+\left(\mu_a V_a'+\mu_b V_b'+\mu_c V_c'\right)VH\frac{\partial H}{\partial t}\right]^2}}{A}\right. \\ &\quad \left.+\frac{\sqrt{\left[\left(\mu_a V_a'+\mu_b V_b'+\mu_c V_c'\right)VH\frac{\partial H}{\partial n}\right]^2}}{A}\right\} \end{aligned} \quad (16)$$

Where, K is the Preston coefficient, which is constantly under fixed finishing conditions; P denotes the pressure applied to the workpiece by the MSTF media; v is the velocity of MSTF media relative to the target surface; N and d are the number of magnetic abrasives participating in the finishing process and the diameter of finishing tool, respectively; n and v_f are the spindle rotational speed of finishing tool and the feed rate of the workpiece, respectively.

Eq. (16) shows that the magnitude of the MRR is not only related to the MSTF media and the workpiece, but also to the magnetic field intensity and magnetic field gradients in finishing zone.

4 Design of finishing tool

In the finishing process, the finishing tool is employed to generate the target mag-netic field in finishing zone. According to Eq. (16), the effectiveness of the finishing process is affected by the performance of magnetic field in the finishing zone. There-fore, it is significant to design an optimal finishing tool to provide enough magnetic flux density and magnetic field gradients in

the finishing zone. To solve the poor uniformity of surface quality when the single cylindrical magnetic pole magnetized along the axial direction were used as the finishing tool. Zou et al. [25] improved the question by optimizing the trajectory of the magnetic brush movement. When a cylindrical magnetic pole magnetized along the radial direction is employed in the finishing process, the relative motion speed is consistent between the magnetic abrasives and every location of the target surface, which greatly improves the uniformity of sur-face quality, as shown in Fig.1(a). Teng et al. [26] greatly improved the magnetic field performance of the finishing zone by slotting the magnetic pole. Therefore, slot-ting for the radial magnetic pole is taken into account in the design of the magnetic field generating device. Nd-Fe-B (Neodymium-Iron-Boron) of grade N38SH was adopted because of the high remanent magnetization and working temperature. The design of the optimal finishing tool was discussed in two steps as follows. Firstly, the size of the radial magnetic pole was determined, then the dimension and quantity of the slots also need to be determined.

4.1 Dimension of radial magnetic pole

It is necessary to calculate the size of the cylindrical radial magnetic pole to guarantee enough magnetic flux density in the finishing zone. Based on first law of magnetic circuit and Kirchhoff's law, the diameter and length of the cylindrical radial magnetic pole are calculated using the following formulas [17].

$$D_m = K_r H_g L_g \sqrt{\frac{B_r}{H_c (BH)_{\max}}} \tag{17}$$

$$S_m = K_f H_g S_g \sqrt{\frac{H_c}{B_r (BH)_{\max}}} \tag{18}$$

Where, D_m is the diameter of radial permanent magnetic, S_m is the effective cross sectional area at working surface. K_f and K_r are the reluctance coefficient and leakage flux coefficient, respectively. L_g and S_g are air gap and cross sectional area of the air gap, respectively. H_g is magnetic field intensity at the air gap. H_c is the coercivity and B_r is the remanent magnetic induction of permanent magnetic. $(BH)_{\max}$ is the maximum energy product of permanent magnetic pole.

By combining the calculation results and the actual processing requirements, the diameter and length of the cylindrical radial magnetic pole were determined as 10 mm and 30 mm, respectively.

4.2 Quantity of radial magnetic pole slots

Eq. (15) shows that the finishing force acting on the MSTF media is related to the magnetic flux density and the magnetic field gradients in the finishing zone. When the radial magnetic pole is slotted, the working gap between the radial magnetic pole and the target surface changes continuously in the finishing process with the rotation of radial magnetic pole. Magnetoresistance is a positive correlation function of the working gap. Hence, a smaller working gap strengthen the magnetic flux density in the finishing zone, resulting in higher magnetic field gradients in the circumferential direction of the radial magnetic pole. The improvement of the magnetic field gradients which increases the magnetic field force acting on the MSTF media. The magnetic force enforces the magnetic abrasives to form a MSTF media brush, which rotates with the radial magnetic pole to achieve the Sine surface finishing.

Four simulation models with various number of slots were designed based on the FEA. The three-dimensional (3D) simulation results of radial magnetic poles with various number of slots

were carried out in COMSOL environment. The optimal solution was achieved when the depth and width of the slots were same. Considering the size and physical strength of the radial magnetic pole, the depth and width of the slot were set to 1 mm. The dimension and material of the simulation models were same as mentioned above. A magnetic field, applying in the radial direction of cylindrical permanent pole, is selected as the excitation source. The simulation results are shown in Fig. 3, the magnetic flux density and magnetic field gradients at the side of the radial magnetic pole increase as the number of slots increases. On the basis of the FEA simulation results and the material properties of magnetic pole, eight-slots radial magnetic pole was selected as the finishing tool for the finishing experiments.

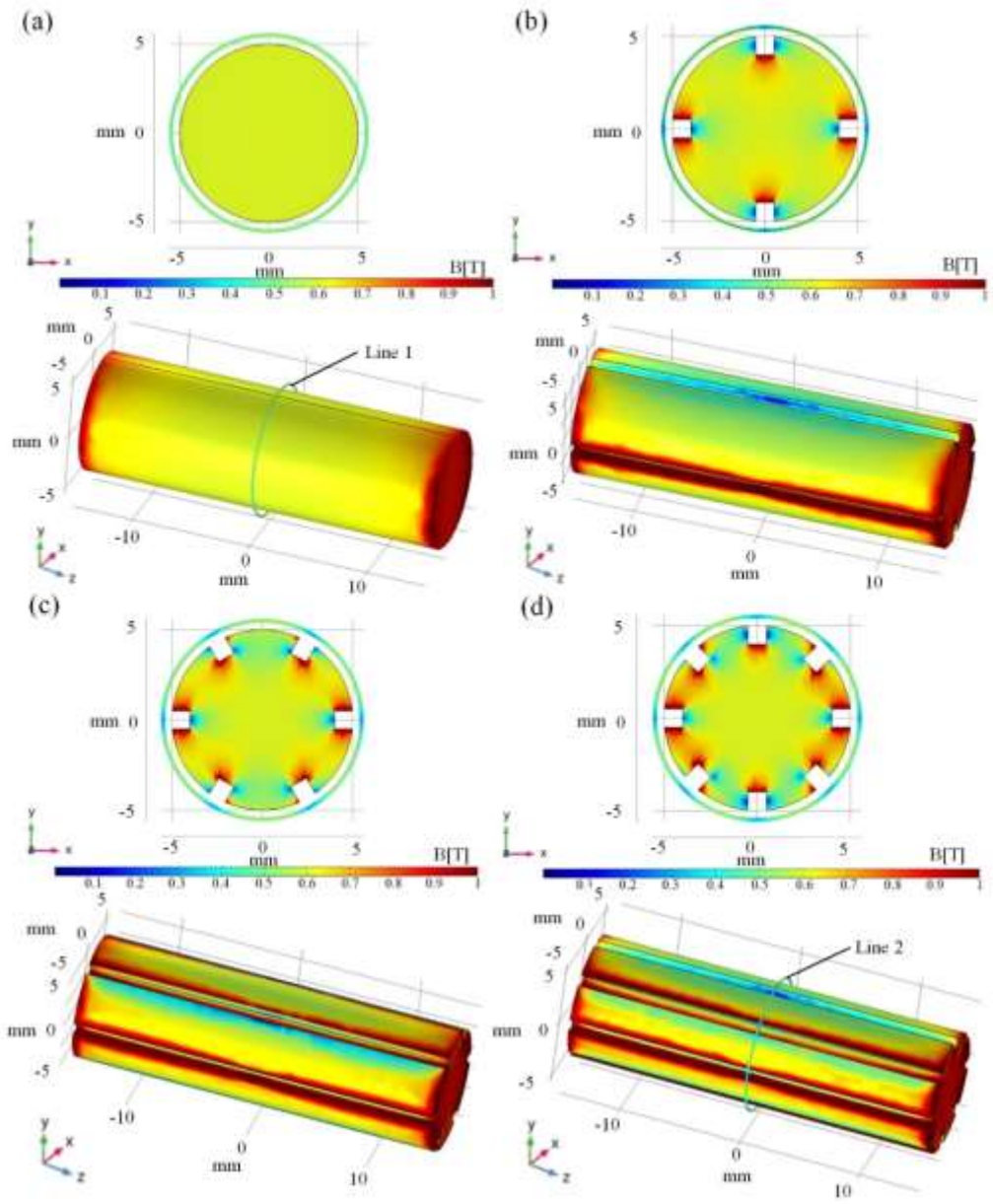

Fig. 3. FEA simulation of magnetic flux density with different number of slots. (a) Non-slotted radial magnetic pole, (b) four-slots radial magnetic pole, (c) six-slots radial magnetic pole, and (d) eight-slots radial magnetic pole

4.3 Fabrication of finishing tool

The brittle fracture defects are easily generated by traditional machining methods because of the NdFeB brittleness. The material is removed by laser thermal fusion, which avoids the hard contact of mechanical processing and guarantees the geometry of the machined workpiece,

because there is no direct contact between the workpiece and the laser generator during laser cutting. Compared to the wire-cut electrical discharge machine (WEDM), laser cutting haves irreplaceable advantages in terms of machinable shape and processing efficiency. Therefore, the designed eight-slots radial magnetic pole was fabricated by a laser cutter (RAYTHER LZ-6060s, China). the detailed machining conditions are listed in Table 1. The physical view of the eight-slots radial magnetic pole is shown in Fig. 4.

Table 1 Laser cutting conditions

Conditions	Value
Cutting speed ($m \cdot min^{-1}$)	2
Laser nozzle height (mm)	2
Gas type	Argon gas
Gas pressure (MPa)	0.5
Peak power (W)	140
Duty Ratio	100%
Pulse frequency (HZ)	2000
Position ofaerodynamic center (mm)	1
Residence time (ms)	200

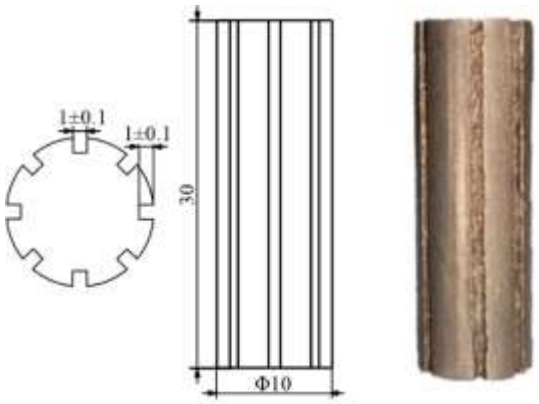

Fig. 4. Physical view of eight-slots radial magnetic pole

4.4 Simulation and measurement of magnetic flux density

To verify the validity of the proposed simulation model, the magnetic flux density of the eight-slots radial magnetic pole was measured. Comparative Experiments were conducted

between the simulation results and experimental measurements. The distributions of magnetic flux density along line 1 and line 2 (Figs. 2(a) and (d)) were analysed using the 3D simulation method. Fig. 5 shows the variation of the magnetic flux density along the circumferential direction at the distance of 0.7 mm from the side for the magnetic pole. The simulation results show that the variation of magnetic flux density along the circumferential direction of the non-slotted radial magnetic pole was unconspicuous. The eight-slots radial magnetic pole generated a large magnetic field gradient along the circumferential direction. A Gauss meter (GM500, China) was employed to verify the validity of the simulation results. The magnetic flux density of the non-slotted radial magnetic pole was smaller than the simulated value due to the magnetic flux leakage in the air. The measured results of the magnetic flux density of the eight-slots radial magnetic pole were smaller than the simulation results, because the high temperature weakens the magnetic performance of the magnetic pole during laser cutting. However, the variation tendency of measurement results was consistent with simulation results, which indicated that machined radial magnetic pole maintained a large magnetic field gradient. The results show that the FEM method is reliable for the magnetic field analysis.

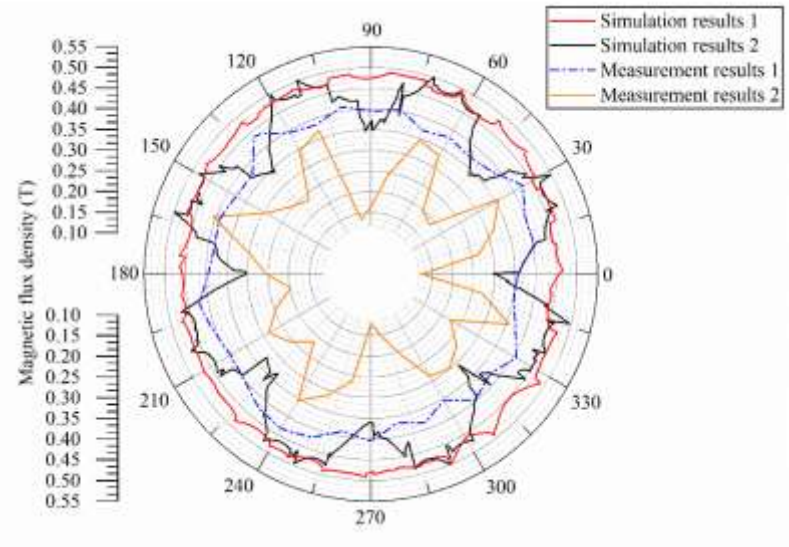

Fig. 5. Comparisons between simulation and experimental measurement

5 Media preparation

The MSTF media was prepared by mixing PEG 200, SiO_2 (diameter 7-40 nm), CIPs and CBN abrasives. The preparation process of the MSTF media was consistent with Fan et al. [16, 27]. PEG 200 was adopted as the base fluids. The fumed SiO_2 particles were gradually dispersed into PEG 200 within 60 min by mechanical stirring with the rotational speed of 350 rpm under the oil bath condition of 80 °C. CIPs and CBN abrasives were added gradually to the mixture with the stirring speed of 350 rpm within 15 min. Finally, the prepared MSTF media was placed in vacuum environment at 25 °C for 1H to remove gas bubbles. The microscopy images of the MSTF media before and after the application of the magnetic field are shown in Fig. 6 based on a digital microscope (OLYMPUS DSX1000, Japan). It was observed that magnetic particles were uniformly dispersed in the mixture (PEG 200 and SiO_2) without obvious directionality. Fig. 6 (b) showed the microstructure of the MSTF media under the action of magnetic field. CIPs were driven by the magnetic field, which was distributed paralleling to the magnetic lines. CBN abrasives were controlled by the formed CIPs structure. Thus, the MSTF media brush with the higher viscosity and stronger bonding force were generated, which improved the finishing force and microscopic material removal.

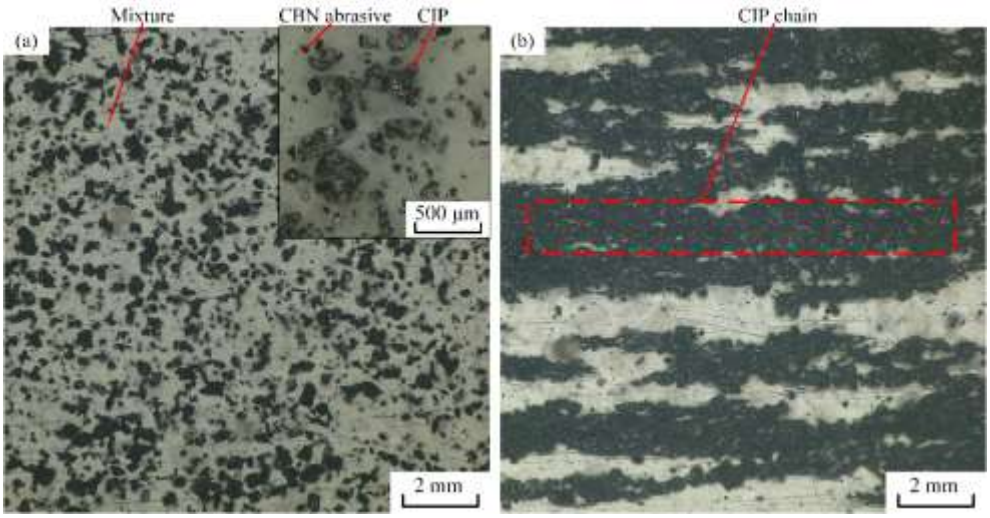

Fig. 6. Microscopy images of the MSTF media. (a) Non-magnetic field, (b) magnetic field action

6 Experimental setup and conditions

As shown in Fig. 7, the experimental system was established to evaluate the feasibility of the MSTF method. An eight-slots radial magnetic pole (size: Φ10 mm×30 mm, the depth and width of the slots: 1 mm) was fixed on the CNC machine center (VERK VKN640, China) spindle. The motion path of the finishing tool could be controlled by the CNC machining center. The workpiece was connected to the dynamometer by a fixture. The dynamometer was connected to data collector and computer for collecting force changes in real time during finishing processes. The workpiece material is SUS304 stainless steel. The target surface is a Sine surface with geometries details as shown in Fig. 7. The initial surface roughness (Ra) of 0.5-0.6 μm was obtained via #80 sand paper grinding. The surface roughness was measured based on an optical profiler (RETC UP-Lamnda, United states).

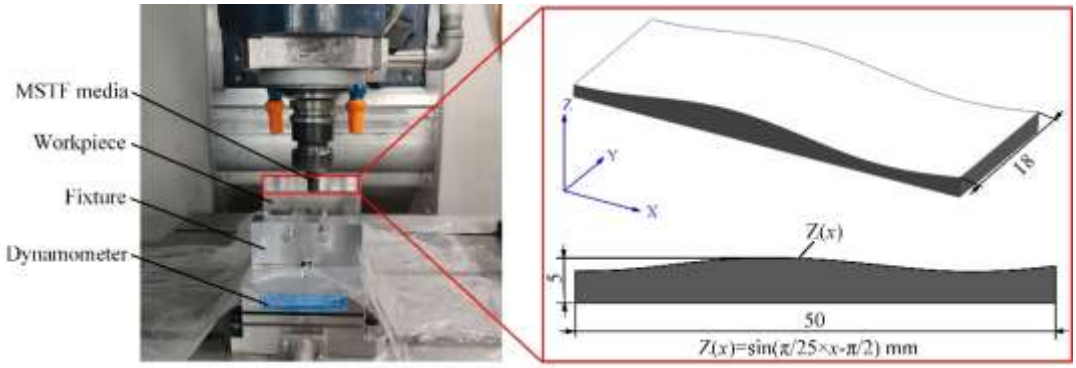

Fig. 7. Prototype of the MSTF system

To explore the finishing performance of the method, five groups of experiments were designed. The first and second groups of experiments were conducted, aiming at evaluating the feasibility of the developed finishing media and finishing tool. Since the critical factors (spindle rotational speed, working gap and magnetic abrasives size) affecting the effect of the MSTF finishing for Sine surface were ambiguous, experiments from third to fifth groups were designed to explore the optimal finishing parameters. According to the Eq. (16), it is evident that the MRR is affected by the configuration of the MSTF media. The volume fractions of CBN abrasives and mixture are inversely proportional to finishing force, increasing the volume fraction of CIPs contributes to the magnetic permeability of the MSTF media, which in turn improves the MRR. In terms of material removal mechanism, CBN abrasives are the main power involved in cutting workpiece peaks. Comprehensive considerations, The MSTF media is composed of CIPs, CBN abrasives and mixture (SiO_2: PEG 200 (wt%)=3: 17), the ratio of mass is 2: 12: 21 respectively. The detailed experimental conditions are listed in Table 2.

Table 2 Experimental conditions

Items	parameters
Spindle rotational speed (rpm)	600, 800, 1000
Working gap (mm)	0.7, 0.9, 1.1
Feed rate (mm/min)	6
Workpiece material	SUS304
Iron particle	CIP

Abrasive	CBN
CIPs size (μm)	150, 50, 5
CBN abrasives size (μm)	106, 23, 2.6
Weight ratio (CIPs: CBN)	6:1
Weight ratio (CIPs and CBN: mixture)	2:3
Mixture concentration (wt %)	15
Surface initial roughness Ra (nm)	500-600

7 Results and discussion

7.1 Effect of varying finishing media

The finishing media plays a vital role in the finishing process, which strongly affects the achievable surface roughness. To verify the effectiveness of the MSTF media, a comparative experiment was conducted. The based fluids of three finishing medias were prepared using mixture (PEG200 & SiO_2), No. 68 lubricating oil and deionized water, respectively. The sizes of CIPs and CBN abrasives were 150 μm and 106 μm, respectively. The experiments were conducted under the motion of combining 1000 rpm spindle rotational speed and 0.7 mm working gap.

Fig. 8 showed that the prepared MSTF media was effective for surface finishing comparing with other two groups. The surface roughness decreased rapidly in initial 30 min for three finishing media. The surface roughness was decreased from 583 nm to 224 nm using the MSTF media, which improved over 61.5%. The MSTF media resulted in higher efficiency in initial 30 min, because the shear-thickening effect generated the higher viscosity and shear stress, which improved the finishing force and the MRR. The No. 68 lubricating oil and deionized water solution without shear thickening effect were adopted to set as contrast experiments to verify the valid of the MSTF media in SUS304 Sine surface finishing. The lower finishing efficiency was observed in both experimental groups using No. 68 lubricating oil and deionized water respectively. The results confirmed that the developed MSTF media contributed to improve the

surface finishing for SUS304 Sine surface. There existed a saturated value of 135 nm for surface roughness from initial 583 nm at the finishing time of 70 min.

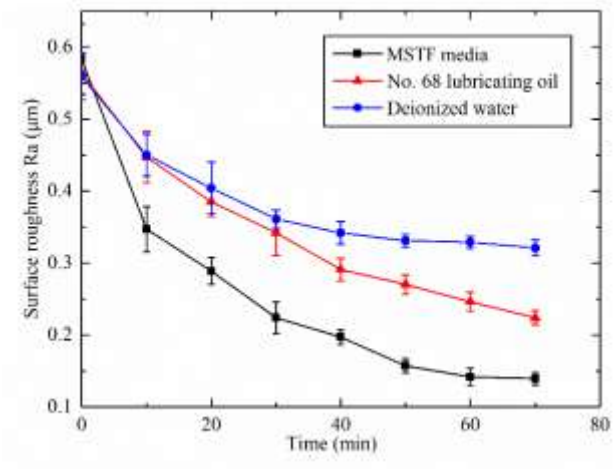

Fig. 8. The variation of surface roughness with the finishing time using varies finishing media

To further investigate the characteristics of finishing process under different finishing media, the finishing force was measured. As shown in Fig. 7, the dynamometer system consisted of a fixed dynamometer (9257B Kistler Instruments Pte Ltd, Switzerland), Charge Amplifier (5167A Kistler Instruments Pte Ltd, Switzerland) and Data Acquisition Unit (5697A Kistler Instruments Pte Ltd, Switzerland). The force measurement range was set to 50 N and the resolution was -7.5 Pc/N. Data acquisition was conducted with the acquisition interval of 10 s. The measurement results are shown in Fig. 9. It was observed that the finishing force using the MSTF media was much larger than the others. The finishing force was 8 N using the MSTF media, the finishing forces were 2 N using No. 68 lubricating oil or deionized water. The finishing force using No. 68 lubricating oil was slightly greater than that of deionized water because of the higher coefficient of friction. The low finishing force results in a low MRR based on the Eq. (16), which weakens the finishing efficiency. The above analysis in the correlation between the finishing force and surface roughness was verified and the MSTF media was valid for Sine surface finishing.

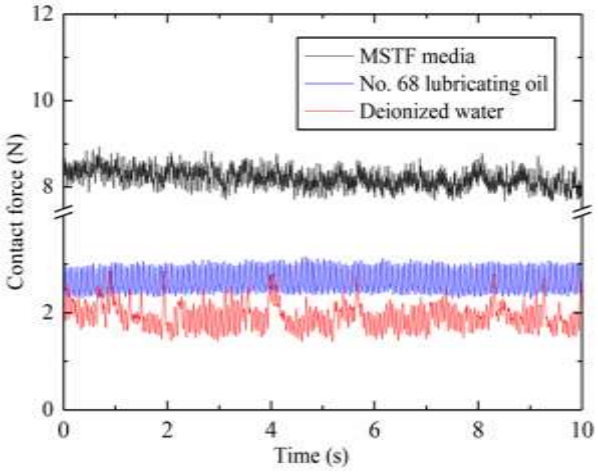

Fig. 9. Finishing force measurement results using varies finishing media

7.2 Effect of varying finishing tools

To verify the effectiveness of the developed finishing tool, finishing experiments were conducted using different finishing tool. The MTSF media with 150 μm CIPs and 106 μm CBN abrasives size was adopted. The spindle rotational speed was 1000 rpm and the working gap was 0.7 mm. Fig. 10 shows the change curve of surface roughness for Sine surface with finishing time using various finishing tools. It was observed that the surface roughness dropped with increasing finishing time when the non-slotted magnetic pole was employed. Its decreasing rate was significantly lower than that in the slotted magnetic pole case. The radial slotted magnetic pole provided large magnetic field gradients in the finishing zone. According to the Eqs. (15) and (16), the MSTF media brush exerted a big finishing force on the target surface, which resulted in the large removal of material. The big finishing force also accelerated the regenerating of ultra-rough surfaces.

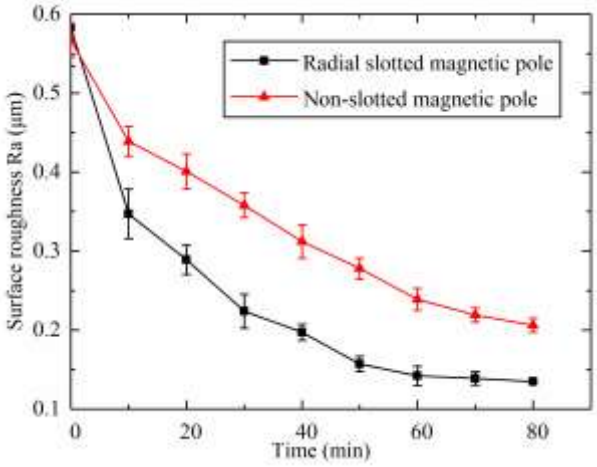

Fig. 10. The variation of surface roughness with the finishing time using varies finishing tools

To illustrate the correlation between the finishing force and magnetic field gradients in the finishing zone, the measurements of finishing force were conducted as shown in Fig. 11. The result showed that the finishing force generated by radial slotted magnetic pole was larger than that in radial non-slotted magnetic pole case, which had good agreement with the simulation results. Meanwhile, the feasibility of the FEA method for the developed finishing tool was verified by the force measurements.

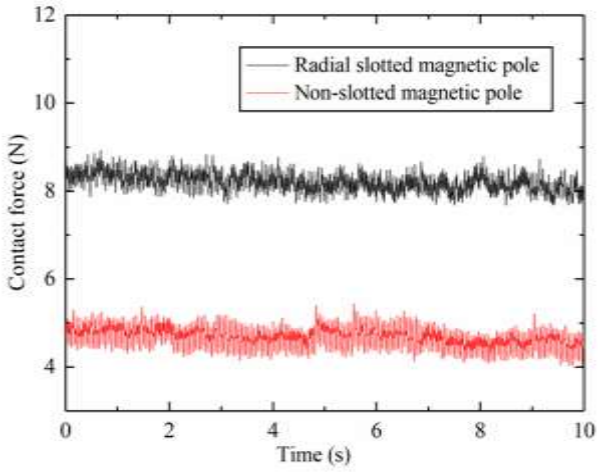

Fig. 11. Finishing force measurement results using varies finishing tools

7.3 Effect of varying the size of magnetic abrasives

It is found that the average particle size of CIPs and CBNs are important parameters, which affects the finishing force and the MRR based on Eqs. (15) and (16). According to the configuration of the MSTF media, three groups of finishing experiments were designed with different sizes of CIPs and CBN abrasives, as shown in Table 3. The other parameters were constant with the following settings. The working gap was 0.7 mm, the spindle rotational speed was 1000 rpm.

Table 3 Particles size of magnetic abrasives in the MSTF media

CBN (μm)			CIP (μm)		
2.6	23	106	5	50	150
3	2	1	3	2	1

Fig. 12 shows that the curves of surface roughness changes with three groups of the MSTF media. A smaller surface roughness was obtained in large magnetic particle size than in small particle size case. The surface roughness of the experimental group 1 was decreased from original 583 nm to 135 nm after 60 min finishing, improving over 76.8%. The results indicated that the large magnetic abrasives (CIPs and CBN abrasives) were grasped easily by the particles cluster compare to the small size, as shown in Fig. 1(b). Meanwhile, the large magnetic abrasives provided large finishing force, which contributed to contacting with ultra-rough surface to improve the MRR. This was consistent with Eq. (16).

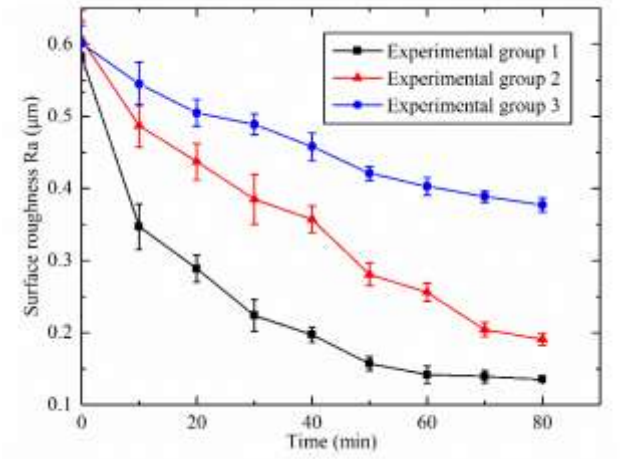

Fig. 12. The variation of surface roughness with the finishing time using various CIPs and CBN abrasives size

7.4 Effect of varying spindle rotational speed

The relative motion between the target surface and the MSTF media brush was generated by the rotation of the finishing tool, which was significant factor affecting the surface roughness based on Eq. (16). Three spindle rotational speeds were used in the experiments, including 600 rpm, 800 rpm and 1000 rpm. The other parameters were constant with the following settings. The working gap was 0.7 mm, the employed MSTF media composed with CIPs and CBN abrasives size distributions of 150 μm and 106 μm. Fig. 13 stated the variation of surface roughness with finishing time at various spindle rotational speeds. The plots depicted that there was a high correlation between the decrease in surface roughness and the increase in spindle rotational speed. After 60 min finishing with the 1000 rpm spindle rotational speed, the surface roughness showed dramatic reduction (75.9%) comparing with the rotational speeds of 800 rpm (66.8%) and 600 rpm (60.5%), which indicated that the finishing efficiency was improved with the increase of spindle rotational speed. Finally, the surface roughness of 127 nm was obtained from the initial 583 nm under the spindle rotational speed of 1000 rpm. According to Eq. (16), the relative velocity is positively related to the MRR. The number of contacts between magnetic abrasives and the target surface are raised with the increase of spindle rotational speed in the same finishing time, which improves the finishing efficiency and surface quality.

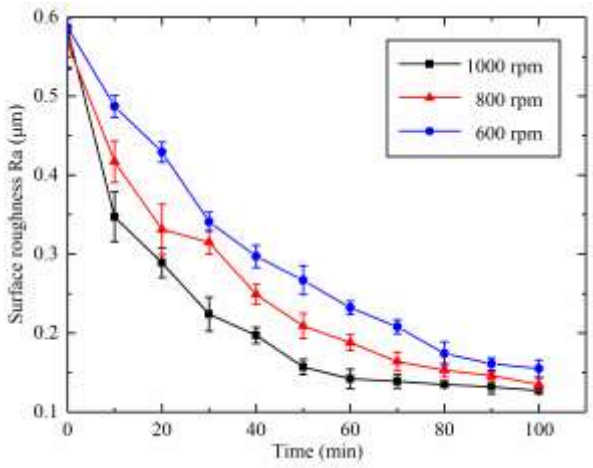

Fig. 13. The variation of surface roughness with the finishing time at various spindle rotational speeds

7.5 Effect of varying working gap

The magnetic flux density in the finishing zone is dominated by changing the working gap. To further explore the effect of the working gap on the magnetic flux density in the finishing zone, the FEM simulation model was established. The trend of magnetic flux density evolution with various working gaps was shown in Fig. 14. The magnetic flux density decreased rapidly with the increase of working gap. Finishing experiments were conducted to investigate the effect of magnetic flux density on surface roughness. The spindle rotational speed was 1000 rpm, the other finishing conditions was same as previous settings. Fig. 15 showed the variation of the surface roughness under three working gaps. It was found that the surface roughness dropped rapidly under the 0.7 mm working gap. The surface roughness reduced from 583 nm to 327 nm after initial 10 min finishing. As comparisons, the other two experimental groups had a relatively lower magnetic flux density under lager working gap, which lead to smaller finishing force and the MRR based on Eqs. (15) and (16). The reshaping speed of the target surface was relatively weaker and the smaller decrease decline in surface roughness was generated with the finishing time. The final of surface roughness of 139 nm, 198 nm, 359 nm were obtained under 0.7 mm, 0.9 mm and 1.1 mm working gap, respectively.

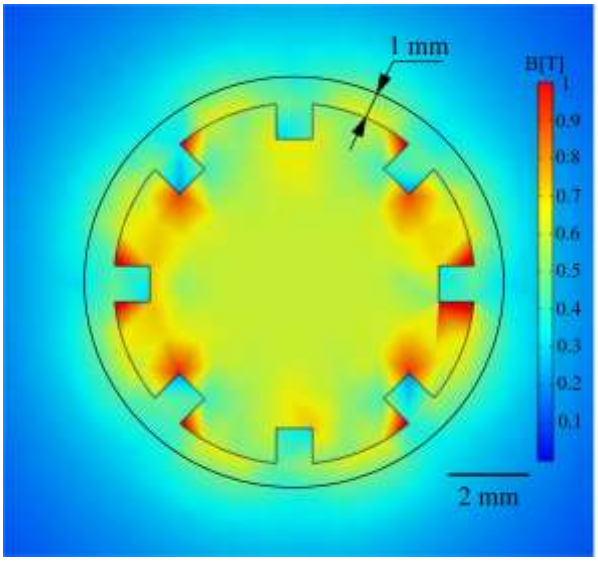

Fig. 14. Simulation results of the magnetic flux density in the cross section

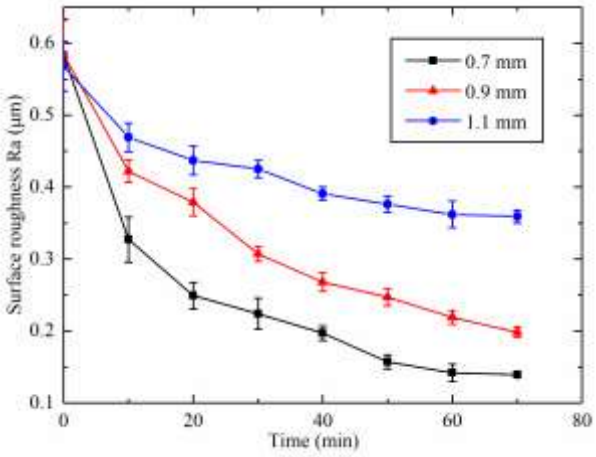

Fig. 15. The variation of surface roughness with the finishing time at various working gaps

7.6 Performance analysis of the finished surfaces

To further verify the feasibility of the Sine surface finishing based on the MSTF method, the surface contour and surface texture were observed by an optical Profiler (Rtec UP-Lamnda, United states) and a field-emission scanning electron microscopy (FEI Sirion 200, United states), respectively. Fig. 16 showed the prototype of workpiece before and after finishing. A mirror surface was successfully generated after rough and fine finishing. The surface roughness (Sa) was 957 nm before finishing. The MSTF media (150 μm CIPs and 106 μm CBN abrasives) was used

in rough finishing. After 60 min of rough finishing, the surface roughness was reduced to Sa 235 nm under the spindle rotational speed of 1000 rpm, working gap of 0.7 mm and feed rate of 6 mm/min. The MSTF media (5 μm CIPs and 2.6 μm CBN abrasives) was prepared for fine finishing, and Sa value of 117 nm was obtained after 30 min finishing. Finally, surface roughness was improved by over 87%. It was obvious that large and deep scratches were visible everywhere. They have been completely removed and replaced by indentations from magnetic abrasives after rough finishing. The surface morphology was still uniform. It was clearly demonstrated that there was an apparent improvement in surface quality of the processed surface. Finally, the indentations were further removed and the surface quality has been greatly improved after 30 min fine finishing, the surface was smoother compared to its initial surface. To ensure the accuracy of the surface shape for the target surface, the surface profiles were measured at the same location with various finishing processes by an optical Profile. Fig. 17 showed that the shape of the Sine surface was consistent before and after the MSTF, which also demonstrated that the method guaranteed the integrity of the Sine surface profile.

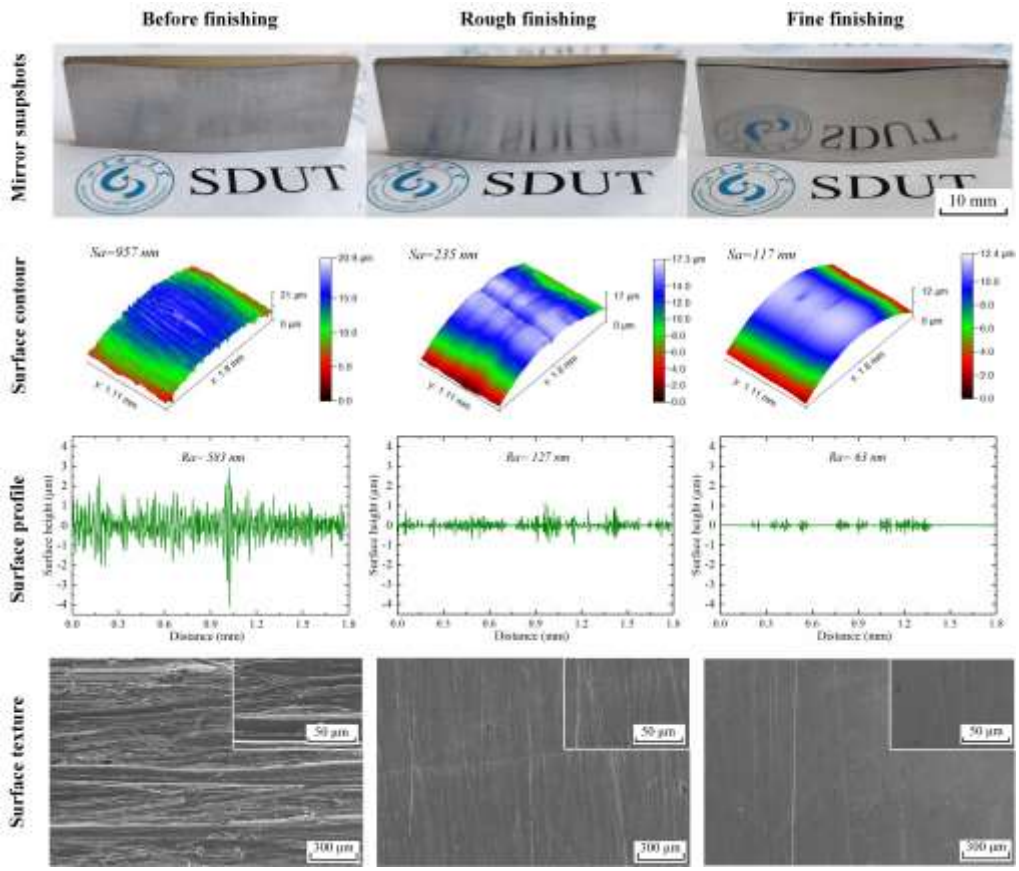

Fig. 16. Surface integrity of the workpiece before and after MSTF

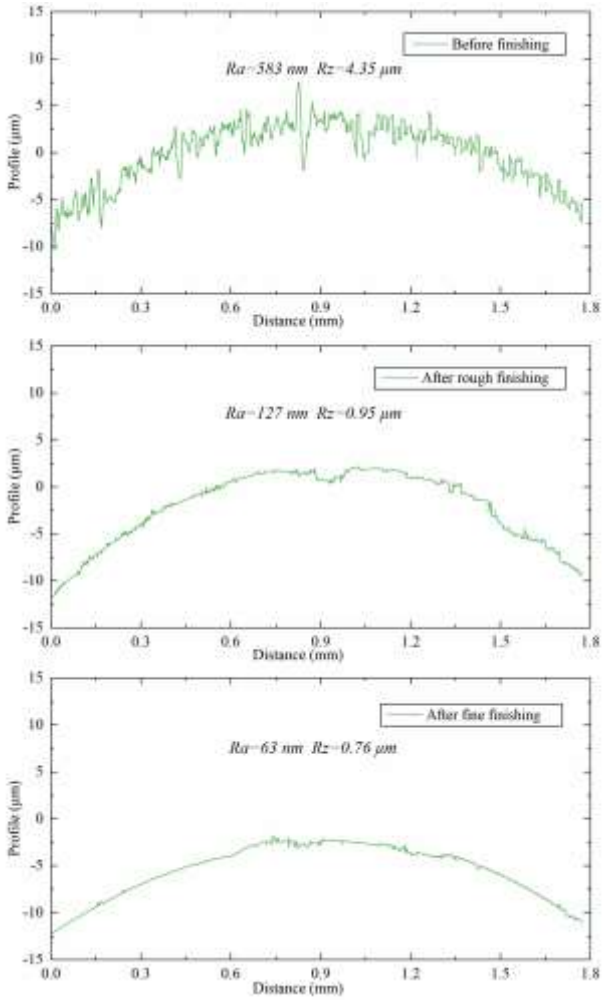

Fig. 17. Analysis of the surface waviness before and after MSTF

8 Conclusions

A novel magnetorheological shear thickening finishing (MSTF) method was proposed for finishing free-form surfaces base on the eight-slots radial magnetic pole and the developed MSTF media in the paper. The FEA method for simulation was employed to obtain the optimal design configuration and size of finishing tool. Mathematical modelling was established to better analysis force characteristics of the MSTF process. Extensive finishing experiments of Sine surface fabricated by SUS304 were conducted to verify the performance of the eight-slots radial magnetic pole and the MSTF media. The effects of the key factors affecting the surface quality,

i.e. the size of magnetic abrasives, the spindle rotational speed and working gap, were also studied. Sine surfaces were investigated in terms of surface morphology observation and surface roughness measurements. The results were used to find out the optimal finishing parameters and validate the feasibility of the established mathematical model. The surface roughness (Sa) was reduced to 117 nm from the initial 957 nm, improving over 87%, after rough and fine surface finishing. Surface morphology observations for target surface further demonstrated that the MSTF method was sufficiently suitable for surface finishing of Sine surface fabricated by SUS304. Finally, a smooth Sine surface without obvious defects was obtain. The findings suggest that the method is feasibility for Sine surface finishing, further researches will be conducted for various shapes and other materials (e.g. titanium alloy, ceramic, etc.).

Funding

This work has been supported by the National Natural Science Foundation of China (Grant No. 51875329 and 51905323), Taishan Scholar Special Foundation of Shandong Province (Grant No. tsqn201812064), Shandong Provincial Natural Science Foundation, China (Grant No. ZR2017MEE050), Shandong Provincial Key Research and Development Project, China (Grant No. 2018GGX103008), Scientific Innovation Project for Young Scientists in Shandong Provincial Universities (Grant No. 2019KJB030), and Key Research and Development Project of Zibo City (Grant No. 2019ZBXC070).

Contribution

Zhiguang Sun: Writing-original draft, Experiment, Investigation, Writing-review and editing, Methodology, Zenghua Fan: Conceptualization, Writing-review and editing, Conceptualization, Yebing Tian: Methodology, Project administration, Funding acquisition, Supervision, Cheng Qian: Investigation, Zhen Ma: Investigation.

Code availability

Not applicable.

Data availability

All authors confirm that all data and materials reported in this paper are available.

Ethics approval

This study complies with the ethical standards set out by Springer. All authors read and approve the final manuscript.

Consent to participate

Not applicable.

Consent for publication

The manuscript is approved by all authors for publication.

Conflict of interest

All authors declare that no conflict of interest exists.

References

[1] Fang FZ, Zhang XD, Weckenmann A, Zhang GX, Evans C (2013) Manufacturing and measurement of freeform optics. CIRP Ann Manuf Tech 62(2):823-846. https://doi.org/10.1016/j.cirp.2013.05.003

[2] Zhang SJ, Zhou YP, Zhang HJ, Xiong ZW, To S, (2019) Advances in ultra-precision machining of micro-structured functional surfaces and their typical applications. Int J Mach Tools Manuf 142:16-41. https://doi.org/10.1016/j.ijmachtools.2019.04.009

[3] Xia ZB, Fang FZ, Ahearne E, Tao M, (2020) Advances in polishing of optical freeform surfaces: A review. J Mater Process Tech 286:116828. https://doi.org/10.1016/j.jmatprotec.2020.116828

[4] Yuan JL, Lyu BH, Hang W, Deng QF, (2017) Review on the progress of ultra-precision machining technologies. Front Mech Eng 12(2):158-180. https://doi.org/10.1007/s11465-017-0455-9

[5] Yung KC, Xiao TY, Choy HS, Wang WJ, Cai ZX, (2018) Laser polishing of additive manufactured CoCr alloy components with complex surface geometry. J Mater Process Tech 262:53-64. https://doi.org/10.1016/j.jmatprotec.2018.06.019

[6] Wu XJ, Kita Y, Ikoku K, (2007) New polishing technology of free form surface by GC. J Mater Process Tech 187–188(1):81-84. https://doi.org/10.1016/j.jmatprotec.2006.11.218

[7] Zhao J, Zhan JM, Jin RC, Tao MZ, (2000) An oblique ultrasonic polishing method by robot for free-form surfaces. Int J Mach Tools Manuf 40(6):795-808. https://doi.org/10.1016/S0890-6955(99)00112-1

[8] Satish K, Jain VK, Sidpara A, (2015) Nanofinishing of freeform surfaces (Knee joint implant) by Rotational - magnetorheological abrasive flow finishing (R-MRAFF) process. Precis Eng 42:165-178. https://doi.org/10.1016/j.precisioneng.2015.04.014

[9] Tam, H, Lui OC, Mok ACK, (1999) Robotic polishing of free-form surfaces using scanning paths. J Mater Process Tech 95(1-3):191-200. https://doi.org/10.1016/S0924-0136(99)00338-6

[10] Qian C, Fan ZH, Tian YB, Liu YH, Han JG, Wang JH, (2021) A review on magnetic abrasive finishing. Int J Adv Manuf Tech 112:619–634. https://doi.org/10.1007/s00170-020-06363-x

[11] Singh RK, Singh DK, Gangwar S, (2018) Advances in Magnetic Abrasive Finishing for Futuristic Requirements - A Review. Mater Today: Proceedings 5(9):20455-20463. https://doi.org/10.1016/j.matpr.2018.06.422

[12] Singh L, Khangura SS, Mishra PS, (2010) Performance of abrasives used in magnetically assisted finishing: A state of the art review. Int J Abras Tech 3(3):215-227. https://doi.org/10.1504/IJAT.2010.034052

[13] Zhang GX, Zhao YG, Zhao DB, Zuo DW, Yin FS, (2013) New Iron-based SiC Spherical Composite Magnetic Abrasive for Magnetic Abrasive Finishing. Chin J Mech Eng 26:377-383. https://doi.org/10.3901/CJME.2013.02.377

[14] Zhang J, Wang H, Kumar AS, Jin MS, (2020) Experimental and theoretical study of internal finishing by a novel magnetically driven polishing tool. Int J Mach Tools Manuf 153:103552. https://doi.org/10.1016/j.ijmachtools.2020.103552

[15] Guo J, Au KH, Sun C, Goh MH, Kum CW, Liu K, Wei J, Suzuki H, Kang RK, (2018) Novel rotating-vibrating magnetic abrasive polishing method for double-layered internal surface finishing. J Mater Process Tech 264:422-437. https://doi.org/10.1016/j.jmatprotec.2018.09.024

[16] Fan ZH, Tian YB, Zhou Q, Shi C, (2020) Enhanced magnetic abrasive finishing of Ti–6Al–4V using shear thickening fluids additives. Precis Eng 64:300-306. https://doi.org/10.1016/j.precisioneng.2020.05.001

[17] Fan ZH, Tian YB, Liu ZQ, Shi C, Zhao YG, (2019) Investigation of a novel finishing tool in mag netic field assisted finishing for titanium alloy Ti-6Al-4V. J Manuf Process 43:74-82. https://doi. org/10.1016/j.jmapro.2019.05.007

[18] Jiao AY, Quan HJ, Li ZZ, Chen Y, (2016) Study of magnetic abrasive finishing in seal ring groo ve surface operations. Int J Adv Manuf Tech 85(5):1195-1205. https://doi.org/10.1007/s00170-01 5-8029-7

[19] Singh AK, Jha S, Pandey PM, (2011) Design and development of nanofinishing process for 3D s urfaces using ball end MR finishing tool. Int J Mach Tools Manuf 51(2):142-151. https://doi.org/ 10.1016/j.ijmachtools.2010.10.002

[20] Guo J, Feng WH, Jong HJH, Suzuki H, Kang RK, (2020) Finishing of rectangular microfeatures by localized vibration-assisted magnetic abrasive polishing method. J Manuf Process 49:204-213. https://doi.org/10.1016/j.jmapro.2019.11.026

[21] Wang CJ, Cheung CF, Ho LT, Yung KL, Kong LB, (2020) A novel magnetic field-assisted mass polishing of freeform surfaces. J Mater Process Tech 279:116552. https://doi.org/10.1016/j.jmatp rotec.2019.116552

[22] Prakash C, Singh S, Pramanik A, Basak A, Krolczyk G, Bogdan-Chudy M, Wu YL, Zheng HY, (2021) Experimental investigation into nano-finishing of β-TNTZ alloy using magnetorheological fluid magnetic abrasive finishing process for orthopedic applications. J Mater Res Tech 11:600-6 17. https://doi.org/10.1016/j.jmrt.2021.01.046

[23] Shinmura T, Takazawa K, Hatano E, Matsunage M, Matsuo T, (1990) Study on Magnetic Abrasi ve Finishing. CIRP Ann Manuf Tech 39(1):325-328. https://doi.org/10.1016/S0007-8506(07)610 64-6

[24] Ming Y, Huang X, Zhou D, Li X, (2022) A novel Non-Newtonian fluid polishing technique for z irconia ceramics based on the weak magnetorheological strengthening thickening effect. Ceram I nt 48(5):7192-7203. https://doi.org/10.1016/j.ceramint.2021.11.280

[25] Zou YH, Xie HJ, Zhang YL, (2020) Study on surface quality improvement of the plane magnetic abrasive finishing process. Int J Adv Manuf Tech 109:1825-1839. https://doi.org/10.1007/s00170 -020-05759-z

[26] Teng X, Zhang GX, Zhao YG, Cui YT, Li LG, Jiang LZ, (2019) Study on magnetic abrasive finis hing of AlSi10Mg alloy prepared by selective laser melting. Int J Adv Manuf Tech 105:2513–25 21. https://doi.org/10.1007/s00170-019-04485-5

[27] Fan ZH, Tian YB, Zhou Q, Shi C, (2020) A magnetic shear thickening media in magnetic field–a ssisted surface finishing. Proc IMechE Part B: J Engineering Manufacture 234(6-7):1069-1072. h ttps://doi.org/10.1177/0954405419896119